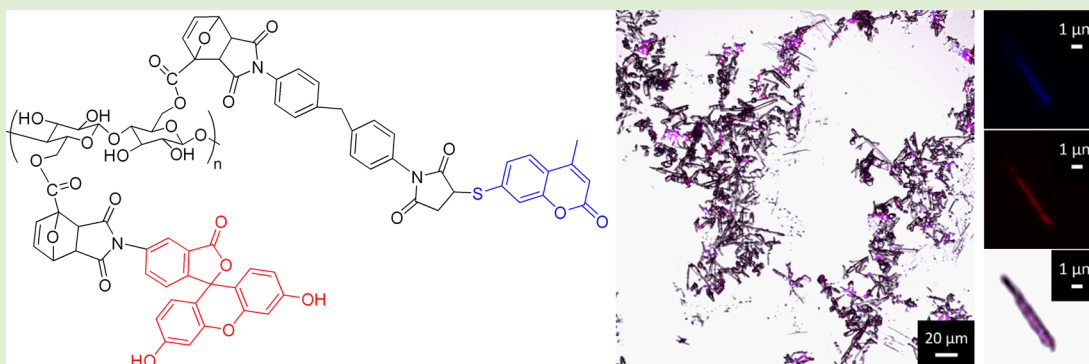


Multicolor Fluorescent Labeling of Cellulose Nanofibrils by Click Chemistry

Julien R. G. Navarro, Guillaume Conzatti, Yang Yu, Andreas B. Fall, Renny Mathew, Mattias Edén, and Lennart Bergström*

Arrhenius Laboratory, Department of Materials and Environmental Chemistry, Stockholm University, Stockholm, Sweden

S Supporting Information



ABSTRACT: We have chemically modified cellulose nanofibrils (CNF) with furan and maleimide groups, and selectively labeled the modified CNF with fluorescent probes; 7-mercapto-4-methylcoumarin and fluorescein diacetate 5-maleimide, through two specific click chemistry reactions: Diels–Alder cycloaddition and the thiol–Michael reaction. Characterization by solid-state ^{13}C NMR and infrared spectroscopy was used to follow the surface modification and estimate the substitution degrees. We demonstrate that the two luminescent dyes could be selectively labeled onto CNF, yielding a multicolor CNF that was characterized by UV/visible and fluorescence spectroscopies. It was demonstrated that the multicolor CNF could be imaged using a confocal laser scanning microscope.

INTRODUCTION

Click chemistry reactions are modular and widely applicable reactions that are characterized by high yield, high atom economy, and in-offensive by-products.^{1,2} There are a number of reactions that qualify as a click chemistry reaction, for example, the azide alkyne cycloaddition using a copper (Cu) catalyst at room temperature.¹ Other important click chemistry reactions are the Diels–Alder (DA) cycloaddition^{3–5} and the thiol–ene reaction.^{6–9} The DA reaction involves a [4 + 2] cycloaddition between a diene and a dienophile while the thiol–ene reaction is the hydrothiolation of a carbon–carbon double bond. The thiol–ene reaction can be performed with either a radical mediated mechanism (thiol–ene), or a base/nucleophilic catalyzed mechanism (thiol–Michael). Click chemistry reactions have been used to modify (bio)polymers for specific applications. Huynh et al.¹⁰ used click chemistry reactions (thiol–ene and thiol–yne) to modify a copolymer and generate, after post-modification, a drug carrier. Pahimanolis et al.¹¹ introduced an azide group onto cellulose and used the click chemistry reaction, with propargyl amine, to produce pH-responsive cellulose.

Fibrillar nanoparticles from cellulose (nanocellulose) have recently attracted significant attention because of the impressive combination of high strength and flexibility. Cellulose nanofibrils (CNF) have been used as a scaffold and reinforcement for

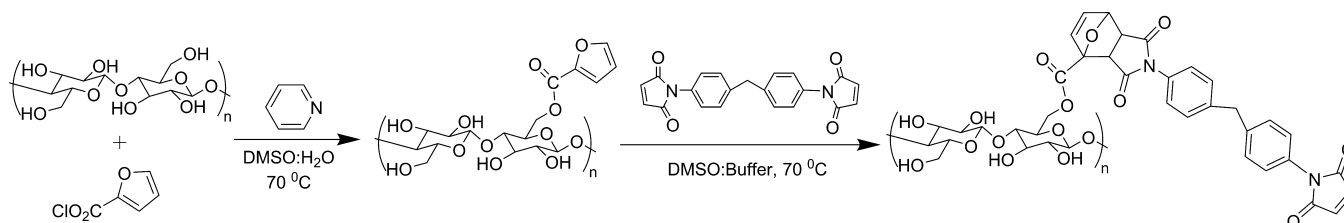
composite films and foams.¹² Surface modification of nanocellulose, for example, by grafting of various types of organic groups, is often required to introduce specific functionalities.^{13–17} Surface modification of nanocellulose has been performed either by, for example, esterification,¹⁸ oxidation,¹⁹ and etherification¹¹ reactions, frequently followed by subsequent post-modifications involving, for example, polymerization,²⁰ photocyclization,²¹ silylation,²² peptidic coupling,²³ and also click chemistry.²⁴

Fluorescent labeling of nanocellulose is of interest in sensor applications.^{25–28} Luminescent CNF are also useful for the study of, for example, cell uptake and cell viability.^{29,30} Huang et al.⁸ functionalized cellulose nanocrystal films with a modified pyrenyl dye using the thiol–ene click reaction. Nielsen et al.³¹ labeled the hydroxide group of the cellulose nanocrystal with either isothiocyanate dyes or succinimidyl ester dyes forming a thiocarbamate or an ester bond, respectively. In all these studies, the fluorescent labeling of nanocellulose was performed through one specific chemical reaction. Introducing several precursors and combining two click-chemistry reactions, for example,

Received: January 20, 2015

Revised: March 11, 2015

Published: March 16, 2015

Scheme 1. Grafting Furan Groups for Diels-Alder Cycloaddition onto Cellulose Nanofibrils^a

^aSurface modification of cellulose nanofibrils through an esterification reaction with 2-furoyl chloride and a Diels-Alder cycloaddition with 1,1'-(methylenedi-4,1-phenylene)bismaleimide.

Diels–Alder cycloaddition and the thiol–Michael reaction, is essential for the development of versatile labeling of nanocellulose with several dyes or other distinct functionalities. Labeling polymer with several species with specific functions or different colors is of great interest for biological application, for example, multimodality molecular imaging,^{32,33} or for studies of electronic energy transfer.³⁴

In this paper, we show that a fluorescein derivative and coumarin can be selectively grafted onto CNF through the Diels–Alder cycloaddition and the thiol–Michael “click” reaction, respectively. The chemical modification and chromophores labeling of the cellulose nanofibrils were monitored by UV/Visible, fluorescence, Fourier transform infrared (FTIR), and magic-angle spinning (MAS) ¹³C nuclear magnetic resonance (NMR) spectroscopies. The distribution of the multicolor-labeled CNF was determined by confocal laser scanning microscopy using different excitation wavelengths appropriate for the two different chromophores.

EXPERIMENTAL SECTION

Materials. 2-Furoyl chloride, 1,1'-(methylenedi-4,1-phenylene)-bismaleimide, fluorescein diacetate 5-maleimide, 7-mercapto-4-methylcoumarin, pyridine, and dimethyl sulfoxide were purchased from Sigma-Aldrich and used as received. All the syntheses and surface modifications were performed using Milli-Q water.

Extraction of Cellulose Nanofibrils (CNF) from Wood Pulp. The nanofibrils were liberated from a bleached and sulfite treated softwood pulp (Domsjö Dissolving Plus). The fibrillation process followed Henriksson et al.³⁵ and includes both an enzymatic pretreatment (endoglucanase) and a series of mechanical treatments (beating and high pressure homogenization). The process resulted in a 1.6 wt % CNF aqueous gel.

Synthesis of Furoate-CNF. The CNF surface modification was adapted from the previously reported protocol^{36,37} with minor modifications. CNF (3.81 g, 1.6% w/w) was suspended in water (5 mL) and the suspension was slowly diluted with an addition of DMSO (80 mL) over a period of 20 min. The solution was then stirred for 4 h at room temperature. 2-Furoyl chloride (5 mL) and pyridine (8 mL) were simultaneously and carefully added, drop by drop, to the suspension. The mixture was allowed to stir for 16 h at 70 °C. Finally, the modified cellulose nanofibrils were purified by centrifugation (6000 rpm/40 min). The supernatant was discarded and replaced with DMSO. The purification steps were repeated six times. The modified CNF was characterized by FTIR spectroscopy and solid-state MAS ¹³C NMR.

Diels–Alder Reaction between Furoate-CNF and 1,1'-(Methylenedi-4,1-phenylene)bismaleimide. Furoate-CNF (1g, 1% w/w) was suspended in 50 mL of DMSO and a sodium phosphate buffer solution was added (pH = 7, 550 μ L). The suspension was stirred for 30 min, followed with an addition of a solution of 1,1'-(methylenedi-4,1-phenylene)bismaleimide in DMSO (100 mg in 10 mL). The mixture was heated up to 70 °C and allowed to react for 48 h. The modified cellulose nanofibrils were purified by centrifugation (6000 rpm/40 min). The supernatant was discarded and replaced with DMSO. The

purification steps were repeated six times. The modified CNF was characterized by FTIR spectroscopy and solid-state MAS ¹³C NMR.

Diels–Alder Reaction between Furoate-CNF and Fluorescein Diacetate 5-Maleimide. The protocol is the same as mentioned before, except that 1,1'-(methylenedi-4,1-phenylene)bismaleimide was replaced with Fluorescein diacetate 5-maleimide (6 mg). The luminescent nanocellulose was purified by centrifugation (6000 rpm/40 min/6 cycles) until a clear supernatant was obtained. To ensure that no unbound chromophores were present in solution, each of the supernatants were analyzed by fluorescence spectroscopy and the purification was continued until no fluorescence signal was detected. The modified CNF was characterized by FTIR, UV–visible, and fluorescence spectroscopy.

Thiol–Michael Reaction between Maleimide-CNF and 7-Mercapto-4-methylcoumarin. Maleimide-CNF (750 mg, 0.25% w/w) was suspended in 50 mL of DMSO and a sodium phosphate buffer solution was added (pH = 7, 550 μ L). 7-Mercapto-4-methylcoumarin (7 mg), in DMSO (3 mL), was added, and the suspension was stirred for 24 h. The luminescent nanocellulose was purified with several centrifugation steps and characterized with FTIR, UV–visible, and fluorescence spectroscopy.

Multicolor Fluorescent Labeling of Cellulose Nanofibrils. The protocol is the same as mentioned before, except that 1,1'-(methylenedi-4,1-phenylene)bismaleimide (20 mg) was added together with fluorescein diacetate 5-maleimide (6 mg). The luminescent nanocellulose was purified by centrifugation (6000 rpm/40 min/6 cycles) until a clear supernatant was obtained. The modified CNF was suspended in 50 mL of DMSO and a sodium phosphate buffer solution was added (pH = 7, 550 μ L). 7-Mercapto-4-methylcoumarin (7 mg), in DMSO, was added, and the suspension was stirred for 24 h. The luminescent nanocellulose was purified with several centrifugation steps and characterized with FTIR, UV–visible, and fluorescence spectroscopy.

Characterization. Infrared spectroscopy was performed using a Varian 610-IR spectrometer, equipped with an attenuated total reflection (ATR) accessory (Specac) and a single-reflection diamond ATR element. Measurements were normally performed by accumulating 64 scans in the spectral region of 4000–390 cm^{-1} with a spectral resolution of 2 cm^{-1} . Absorption spectra were recorded using a PerkinElmer Lambda 19 UV–vis-NIR spectrometer. Fluorescence spectra were obtained using a Varian Cary Eclipse fluorescence spectrophotometer. Confocal laser scanning microscopy imaging was performed with a Zeiss LSM 5 exciter microscope. A diode laser (405 nm) and a HeNe laser (543 nm) were used together with a 63 \times /1.4 NA oil-immersion objective lens, beam splitters (HFT 405/488/543/633), and long-pass filters (420 and 560 nm).

All ¹³C NMR experiments were performed with a Bruker Avance-III spectrometer at an external magnetic field of 14.1 T, which gives Larmor frequencies of −150.9 and −600.1 MHz for ¹³C and ¹H NMR, respectively. The samples were packed in 4 mm zirconia rotors and spun at 14.00 kHz, except for the unmodified CNF that utilized 12.50 kHz. Ramped³⁸ cross-polarization (CP) ¹³C MAS NMR spectra were recorded at the modified Hartmann–Hann condition, $\omega_{\text{nut}}^{\text{H}} - \omega_{\text{nut}}^{\text{C}} = \omega_r$, with a ¹³C nutation frequency of ~40 kHz. CPMAS ¹³C NMR spectra are inherently nonquantitative, because the ¹H → ¹³C magnetization transfer efficiency depends on the ¹H–¹³C internuclear

distance and molecular dynamics.³⁹ On the other hand, owing to the low substitution degree of the cellulose materials, it is not possible to record quantitative NMR spectra of sufficient quality by direct excitation with single pulses. Consequently, to achieve unambiguous evidence of the anchoring of the furan and maleimide molecules onto CNF by MAS NMR in a reasonable time, our experimentation utilized $^1\text{H} \rightarrow ^{13}\text{C}$ CP with a contact time of 1 ms: this emphasizes the ^{13}C NMR signals from ^{13}C featuring direct bonds to protons (such as aromatic carbons), while ^{13}C sites more distant to protons (e.g., the ester group of furoate-CNF) may pass undetected. High-power ^1H decoupling was achieved by the TPPM technique⁴⁰ using a nutation frequency of ~ 75 kHz, a TPPM pulse length of $6.0\ \mu\text{s}$ and a phase difference of 15° between the consecutive pulses of the pair. All NMR acquisitions involved relaxation delays of 4 s, whereas 4096, 16348, and 24576 signal transients were accumulated for unmodified-CNF, furoate-CNF, and maleimide-CNF, respectively. Signal apodization by an 80 Hz Lorentzian broadening was applied before Fourier transformation and ^{13}C chemical shifts are quoted relative to neat tetramethylsilane (TMS).

RESULTS AND DISCUSSION

The cellulose nanofibrils CNF were first chemically modified for further click-chemistry surface modification and then labeled with luminescent probes. Furan groups were introduced by reacting the hydroxyl group on the C-6 position on the nanocellulose backbone with 2-furoyl chloride in the presence of pyridine, in a DMSO/ H_2O mixture, as shown in Scheme 1. This results in the covalent attachment of the furan-containing unit through the formation of an ester bond.^{37,41}

The furoate-CNF reaction was performed in the presence of pyridine. Pyridine played the role of the acid scavenger for the generated HCl, which needs to be neutralized to avoid hydrolysis of the ester. Pyridine may also react with the 2-furoyl chloride to form an unstable complex (acylpyridinium salt) that has been shown to be a good leaving group for esterification.⁴² The furoate-CNF was purified through several centrifugation steps where the supernatants were removed.

Diels–Alder (DA) cycloaddition was performed between the furoate-CNF and 1,1'-(methylenedi-4,1-phenylene)-bismaleimide, as shown in Scheme 1. The reaction was carried out at 70°C in a mixture of sodium phosphate buffer ($\text{pH} = 7$) and DMSO to avoid hydrolysis of the furoate-CNF ester bond. The 1,1'-(methylenedi-4,1-phenylene)bismaleimide was used in large excess to promote surface modification and minimize cross-linking of CNF.³⁶

Figure 1 compares infrared (IR) spectra of unmodified CNF with IR spectra of furoate-CNF and maleimide-modified CNF. Figure 1b shows that furoate-CNF exhibit infrared bands localized at $1701\ (\text{C}=\text{O})$, $1107\ (\text{C}-\text{O}$ in furan ring), 1010 (ring breathing),⁴³ and $757\ \text{cm}^{-1}$ (monosubstituted furan ring)⁴⁴ in addition to the characteristic absorption bands of the unmodified CNF (Figure 1a). The IR spectra in Figure 1c suggests that the DA cycloaddition was successful as the modified material possess IR bands characteristic of the maleimide molecule: $1701\ (\text{C}=\text{O})$, 1510 – $1360\ (\text{C}=\text{C}$, aromatic), $1157\ (\text{C}-\text{N}$, maleimide), and $994\ \text{cm}^{-1}\ (\text{C}-\text{H}$, aromatic).^{45–47}

Figure 2 shows CPMAS ^{13}C NMR spectra recorded from unmodified CNF, as well as the partially substituted furoate-CNF and maleimide-modified CNF specimens. The NMR spectrum from CNF displayed in Figure 2a agrees well with previous literature reports on unmodified CNF.^{48–50} The various ^{13}C NMR assignments are provided at the top of the spectrum. The signals appearing around 84 ppm and 63 ppm correspond to the carbon sites at the CNF surface, while the signals around 89 ppm

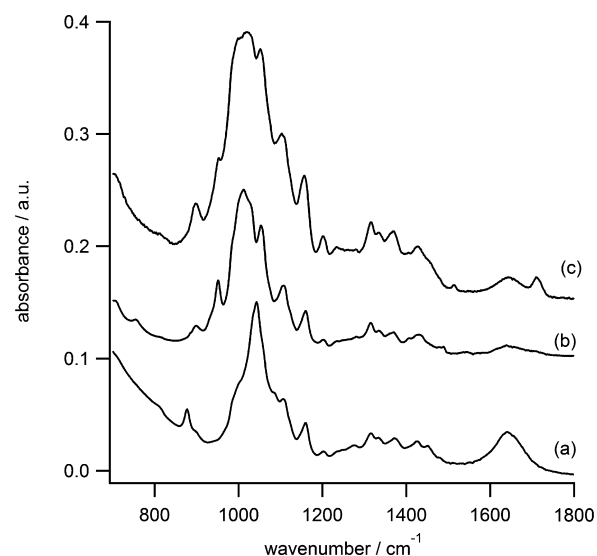


Figure 1. Infrared characterization of surface-modified cellulose nanofibrils (CNF): FTIR spectra of (a) unmodified CNF, (b) furoate-CNF, and (c) maleimide-modified CNF. The curves have been shifted for clarity.

and 66 ppm are attributed to ^{13}C inside the crystalline sections of CNF.⁵¹

Figure 2b,c displays the NMR spectra observed from furoate-CNF and maleimide-modified CNF. Integration of the NMR peaks reveals relatively low degrees of surface grafting of furoate and maleimide, estimated conservatively to amount to $\approx 1\%$. Note that some of the ^{13}C NMR signals of the substituents are not feasible to unambiguously identify as they overlap with the ~ 100 -fold larger main centerband signals from cellulose or their less intense set of spinning sidebands (marked by asterisks in Figure 2). Hence, we only discuss the resonances that may be assigned with reasonable certainty: they all appear in the range 120–150 ppm and are indicated in the zoomed spectral portions shown in Figure 2b,c.

In Figure 2b, the signal at 128 ppm is assigned to site C9 of the furan ring, in accordance with high resolution ^{13}C NMR data of 2-furoyl chloride in CDCl_3 , whose corresponding signal appears at 125.0 ppm.⁵² The ^{13}C NMR peaks around 142 ppm and 149 ppm are attributed to sites C11 and C8 (although definite assignments cannot be made), based on previous observations⁵³ from ^{13}C solution NMR data of furoate-CNF in $\text{DMSO}-d_6$. Köhler and Heinze⁵³ showed that the ^{13}C NMR signals from C7 and C10 of furan are expected to appear around 157 ppm and 112 ppm, respectively, and would thereby overlap with the dominating resonances from cellulose. Moreover, as discussed in the Experimental Section, our MAS NMR conditions are nonoptimal for exciting the ^{13}C site of the nonprotonated ester group. The ^{13}C NMR spectrum from maleimide-CNF (Figure 2c) reveals primarily a broad signal around 128 ± 3 ppm in the region where resonances from the maleimide molecule are expected to appear. The present solid-state NMR results are commensurate with reported high-resolution ^{13}C NMR data of 1,1'-(methylenedi-4,1-phenylene)bismaleimide in CDCl_3 , whose aromatic sites predominantly manifest ^{13}C chemical shifts in the range of 126–130 ppm.⁵⁴

Two different luminescent probes were selectively grafted onto the surface-modified CNF. Scheme 2 illustrates how fluorescein diacetate 5-maleimide was labeled onto furoate-CNF through the Diels–Alder cycloaddition and how 7-mercapto-4-

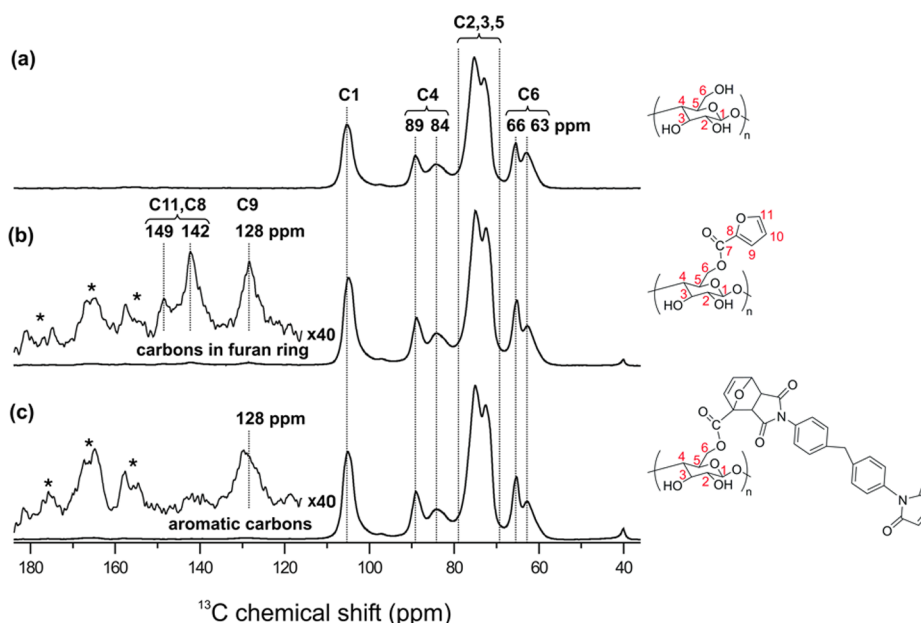


Figure 2. Solid-state NMR characterization of surface-modified cellulose nanofibrils: CPMAS ^{13}C NMR spectra of (a) unmodified CNF, (b) furoate-CNF, and (c) maleimide-modified CNF. The corresponding molecular structures of the CNF and the surface modified CNF are shown in the right panel. The insets in (b) and (c) display zooms over the spectral region 116–184 ppm, with some identified signals from the substituents indicated. Spinning sidebands are marked by asterisks.

methylcoumarin was labeled onto maleimide-modified CNF by the thiol-Michael reaction.

Figure 3a shows that a solution of fluorescein diacetate 5-maleimide display an absorption band in the UV-range localized at 290 nm. However, when the fluorescein diacetate 5-maleimide is reacted with 2-mercaptoethanol (thiol-Michael click reaction with the maleimide group) in a mixture of phosphate buffer and DMSO (hydrolysis of the acetate group), the resulting chromophore (fluorescein reference product) absorption-emission bands are shifted to the visible region with peaks localized at 496 and 541 nm. For a better comparison and to highlight the bands shift, both of the absorption and emission spectra (Figure 3a) were rescaled with respect to the maximum intensity. It is important to note that the solution is only fluorescent when the thiol-Michael reaction (with 2-mercaptoethanol) and the hydrolysis of the acetate groups has been performed, suggesting that both acetate and maleimide groups are fluorescent quenchers. Figure 3b shows that fluorescein-modified CNF, display a small red-shift compared to the fluorescein reference product; the absorption band shifts from 496 to 519 nm, and the emission band shifts from 530 to 541 nm. Indeed, the red-shifts of chromophores labeled onto CNF has been reported previously and was attributed to the covalently grafted chromophores onto CNF.^{30,55}

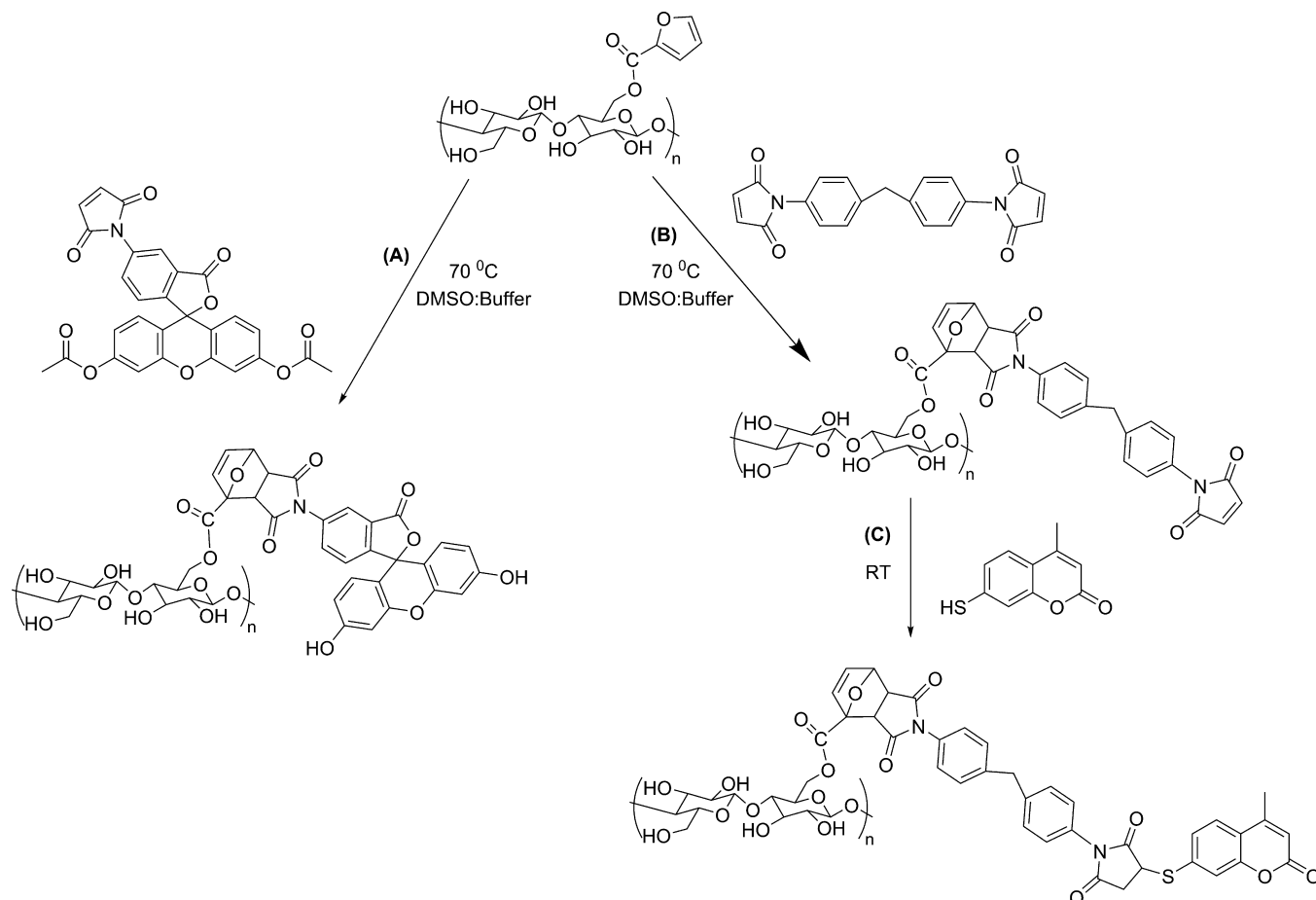
Figure 4a shows that the absorption spectrum of 7-mercapto-4-methylcoumarin in DMSO is composed of two absorption bands localized in the visible region at 327 and 436 nm. Previous work has shown that the photophysical properties of this dye is highly dependent on the reaction media;⁵⁶ in acidic condition, the absorption band is localized at 327 nm (corresponding to the neutral form of 7-mercapto-4-methylcoumarin (Cm-SH)) while in basic condition the band is shifted to 436 nm (corresponding to the anionic form of 7-mercapto-4-methylcoumarin (Cm-S^-)). For a better comparison and to highlight the bands shift, both of the absorption and emission spectrum in Figure 4a were rescaled with respect to the maximum intensity. The existence of two

peaks in Figure 4 thus suggests that 7-mercapto-4-methylcoumarin is present in both forms in DMSO. However, after the thiol-Michael click reaction of 7-mercapto-4-methylcoumarin with 1,1'-(methylenedi-4,1-phenylene)bismaleimide (reference product), only one absorption band was detected at 327 nm. This indicates that no unbound anionic chromophores are present in solution after click-chemistry modification and purification. In the case of the coumarin-based reference product, the maximum of the emission band remain at the same position as for the free neutral form of the coumarin dye. Figure 4b shows that the emission band of the coumarin-labeled CNF is red-shifted (397 nm to 410 nm) compared to the emission band of the reference compound (the thiol-Michael reaction between 7-mercapto-4-methylcoumarin and 1,1'-(methylenedi-4,1-phenylene)-bismaleimide).

We have also fluorescently tagged CNF with both fluorescein and coumarin (FC-CNF) by using a combination of the Diels–Alder cycloaddition and the thiol-Michael reaction pathways, as shown in Scheme 3.

The fluorescence spectra FC-CNF (Figure 5) display two different emission bands in the visible region depending on the excitation wavelength. For better comparison, both emission spectra in Figure 5 were rescaled with respect to the maximum intensity. The emission band at 406 nm is obtained after excitation at 327 nm and can be assigned to the coumarin dye, while coumarin-CNF displayed an emission band at 410 nm (Figure 4b). The emission band at 530 nm (Figure 5) is obtained after excitation at 510 nm and can be assigned to the fluorescein dye, while fluorescein-CNF displayed an emission band at 541 nm (Figure 3b).

We expect that possible shifts of the absorption-emission bands or quenching-enhancement of the fluorescence intensity^{57–60} due to a too close proximity of the grafted chromophores should be small, as the substitution degree of furan and maleimide was shown by solid-state ^{13}C NMR to approximately amount to 1%. Interestingly, while comparing the

Scheme 2. Labeling of Fluorescent Probes onto Surface-Modified Cellulose Nanofibrils (CNF)^a

^a(A) Fluorescent labeling of furoate-modified CNF with fluorescein diacetate 5-maleimide using Diels-Alder cycloaddition, (B) synthesis of maleimide-modified CNF through Diels-Alder cycloaddition between furoate-modified CNF and 1,1'-(methylenedi-4,1-phenylene)bismaleimide, (C) fluorescent labeling of maleimide-modified CNF with 7-mercapto-4-methylcoumarin by the thiol-Michael reaction.

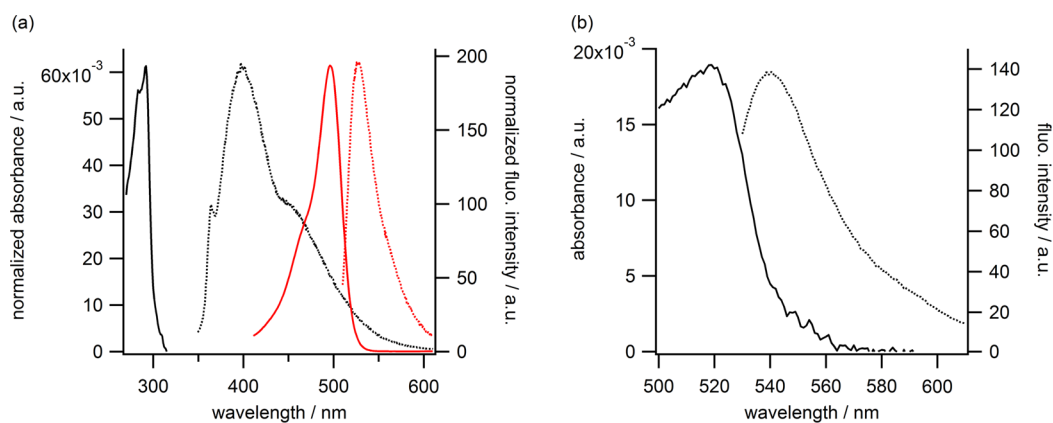


Figure 3. Characterization of fluorescein-labeled cellulose nanofibrils and the precursors. (a) Normalized UV-visible (solid line) and normalized fluorescence spectra (dashed line) of solutions of fluorescein diacetate 5-maleimide (black) and fluorescein reference product (red; after thiol-Michael reaction with 2-mercaptoethanol and hydrolysis of the acetate group). (b) UV-visible (solid line) and fluorescence spectra (dashed line) of fluorescein-labeled CNF.

emission bands position of fluorescein-CNF, coumarin-CNF, and FC-CNF with their respective reference products, the bands position of the multicolour-CNF (406 and 530 nm, FC-CNF) become comparable with the position of the emission band of the reference products (397 and 530 nm). This suggests that labeling of the two dyes onto CNF avoid a dye-to-dye

interaction (for the same chromophore) since the substitution degree is initially low and the distance between two identical dyes may be large if we assume a random distribution of the two chromophores.

Confocal laser scanning microscopy imaging has been performed on drop cast multicolor luminescent FC-CNF

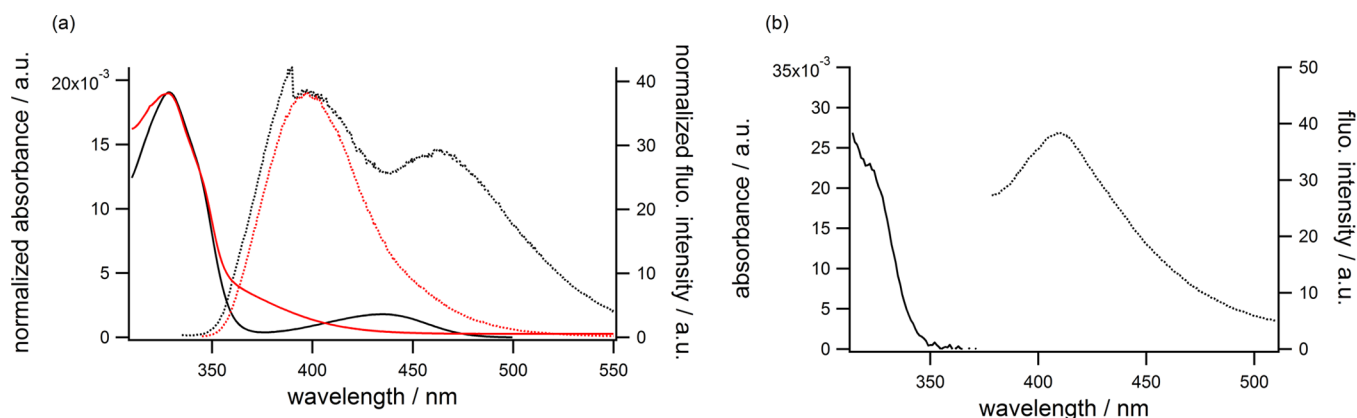
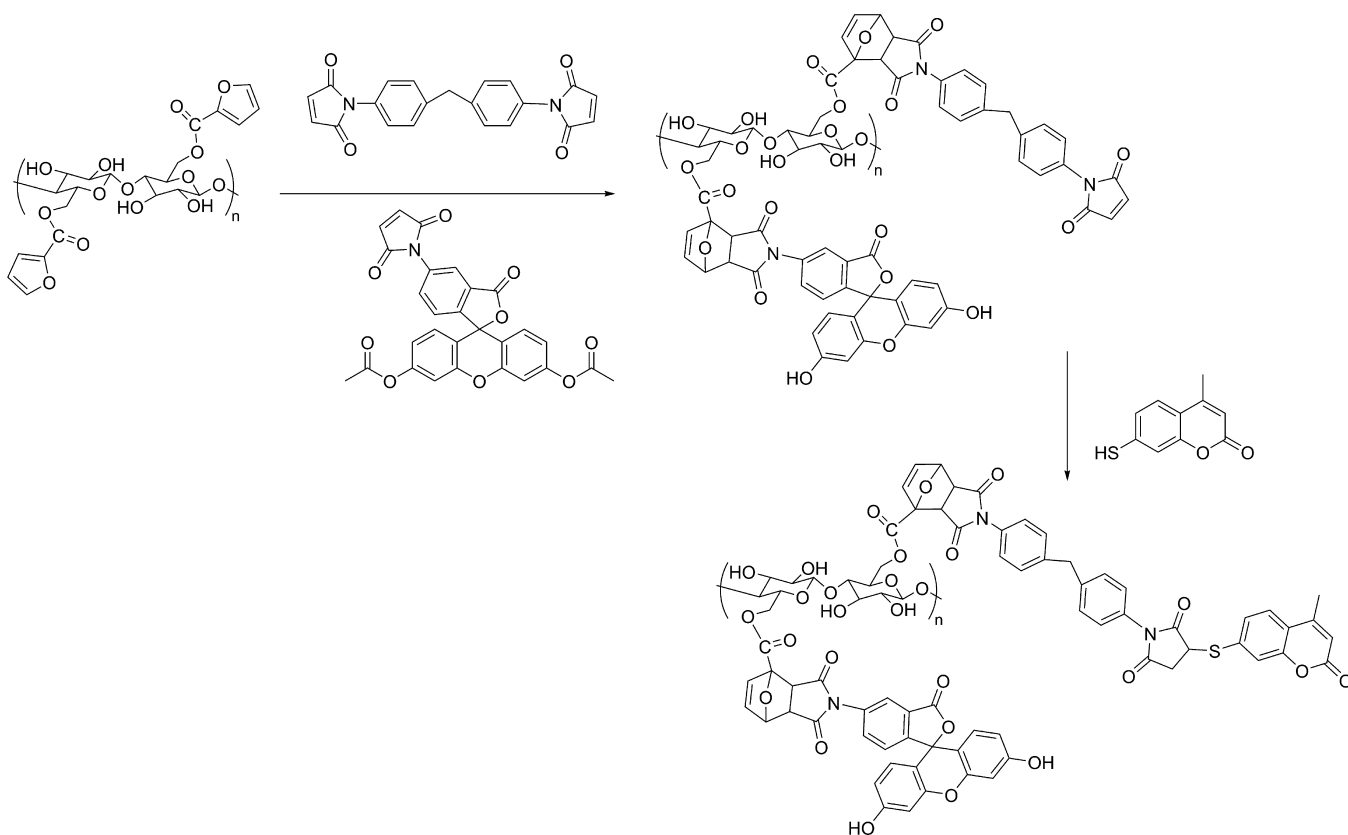


Figure 4. Characterization of coumarin-labeled cellulose nanofibrils and the precursors. (a) Normalized UV–visible (solid line) and normalized fluorescence spectra (dashed line) of solutions of 7-mercapto-4-methylcoumarin (black) and 7-mercapto-4-methylcoumarin reacted with 1,1'-(methylenedi-4,1-phenylene)bismaleimide (red). (b) UV–visible (solid line) and fluorescence spectra (dashed line) of coumarin-CNF.

Scheme 3. Preparation of Multicolor CNF^a



^aLabeling of fluorescein diacetate 5-maleimide and 7-mercapto-4-methylcoumarin through the combination of Diels-Alder cycloaddition and thiol-Michael click reaction.

suspension. The fluorescence images were obtained with two different excitation wavelengths and the combined bright-field fluorescence overlay images are shown in Figure 6. The fluorescence image with a shorter excitation wavelength identifies the position of the coumarin labeling (blue spots), while an excitation at 540 nm showed the position of the fluorescein labeling (red spots). We can clearly see that the distribution of the blue and red luminescent spots is equally distributed and can be overlaid onto the nanocellulose fibers. No free luminescent spots were observed outside the overlaid blue and red region, that is, where the FC–CNF is deposited, which

suggest that the removal of unbound chromophores was successful.

CONCLUSIONS

Cellulose nanofibrils (CNF) have been chemically modified and selectively labeled with two different fluorescent probes (7-mercapto-4-methylcoumarin and fluorescein diacetate 5-maleimide), through two specific click chemistry reactions: Diels–Alder cycloaddition and/or the thiol-Michael reaction. Fourier transform infrared spectroscopy and solid-state ¹³C NMR showed that the first step in the surface modification of CNF

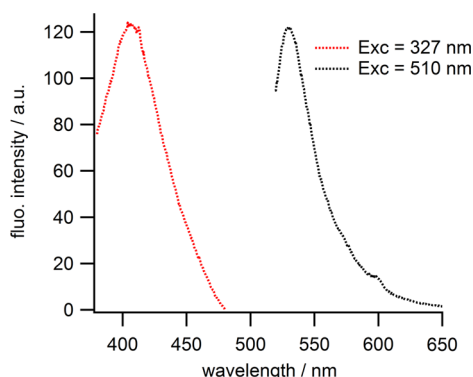


Figure 5. Fluorescence spectra of FC-CNF excited at two different wavelengths: 327 and 510 nm. The red band corresponds to the emission band of the coumarin, while the black band corresponds to the emission band of the fluorescein.

that yields furoate-CNF and maleimide-CNF was successful. The ^{13}C CPMAS NMR data also showed that the substitutions degrees of the two compounds (furoate-CNF and maleimide-CNF) were relatively low and could be estimated conservatively to $\approx 1\%$. The CNF was then labeled with two different chromophores and characterized with fluorescence spectroscopy. In the single dye-CNF case, a red-shift of the emission band was observed (if compared to the respective reference product), while the position of the emission bands of the multicolor CNF become comparable with the emission bands of the reference products. The labeling of two dyes onto CNF avoid a dye-to-dye interaction (for the same chromophore), for example, red shift of the emission band, since the substitution degree is initially low and the distance between two identical dyes may be large enough, while assuming a random distribution of the two chromophores. Multicolor CNF labeled with both coumarin and fluorescein (FC-CNF) was imaged by confocal laser scanning microscopy. Imaging with two different excitation wavelengths enabled the position of the individual dyes to be accurately determined. The excellent correspondences of the overlaid images, also at the highest possible resolution, show that the click-chemistry synthesis yield multicolor labeled CNF with an insignificant amount of free chromophores. The chemical modification of CNF and the selective labeling of fluorescent dyes through different click chemistry reactions are of great

interest for biological application such as multimodality molecular imaging.

■ ASSOCIATED CONTENT

Supporting Information

FTIR spectrum of furoate-CNF in the $1500\text{--}2000\text{ cm}^{-1}$ region. This material is available free of charge via the Internet at <http://pubs.acs.org>.

■ AUTHOR INFORMATION

Corresponding Author

*E-mail: lennart.bergstrom@mmk.su.se.

Notes

The authors declare no competing financial interest.

■ ACKNOWLEDGMENTS

We acknowledge financial support from the Wallenberg Wood Science Center (WWSC). The authors would like to thank Chao Xu and Niklas Hedin for their help with liquid state NMR.

■ REFERENCES

- (1) Kolb, H. C.; Finn, M. G.; Sharpless, K. B. *Angew. Chem., Int. Ed.* **2001**, *40*, 2004–2021.
- (2) Nebhani, L.; Barner-Kowollik, C. *Adv. Mater.* **2009**, *21*, 3442–3468.
- (3) Diels, O.; Alder, K. *Liebigs Ann. Chem.* **1928**, *460*, 98–122.
- (4) Tasdelen, M. A. *Polym. Chem.* **2011**, *2*, 2133–2145.
- (5) Li, M.; De, P.; Gondi, S. R.; Sumerlin, B. S. *J. Polym. Sci., Polym. Chem.* **2008**, *46*, 5093–5100.
- (6) Lowe, A. B. *Polym. Chem.* **2010**, *1*, 17–36.
- (7) Zhao, G.-L.; Hafrén, J.; Deiana, L.; Córdova, A. *Macromol. Rapid Commun.* **2010**, *31*, 740–744.
- (8) Huang, J.-L.; Li, C.-J.; Gray, D. G. *RSC Adv.* **2014**, *4*, 6965–6969.
- (9) Tingaut, P.; Hauert, R.; Zimmermann, T. *J. Mater. Chem.* **2011**, *21*, 16066–16076.
- (10) Huynh, V. T.; Chen, G.; de Souza, P.; Stenzel, M. H. *Biomacromolecules* **2011**, *12*, 1738–1751.
- (11) Pahimanolis, N.; Hipp, U.; Johansson, L.-S.; Saarinen, T.; Houbenov, N.; Ruokolainen, J.; Seppälä, J. *Cellulose* **2011**, *18*, 1201–1212.
- (12) Wicklein, B.; Salazar-Alvarez, G. *J. Mater. Chem. A* **2013**, *1*, 5469–5478.
- (13) Galland, S.; Andersson, R. L.; Salajková, M.; Ström, V.; Olsson, R. T.; Berglund, L. A. *J. Mater. Chem. C* **2013**, *1*, 7963–7972.

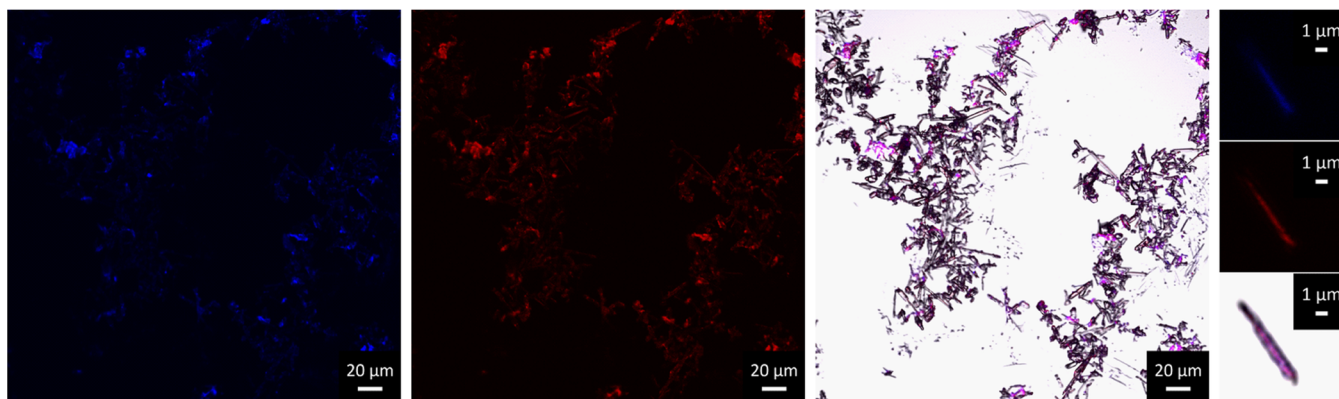


Figure 6. Confocal scanning laser microscopy imaging of fluorescein/coumarin-labeled cellulose nanofibrils (FC-CNF). (a) fluorescence image at an excitation wavelength of 405 nm (relating to coumarin, blue color), (b) fluorescence image at an excitation wavelength of 540 nm (relating to fluorescein, red color), and (c) combined overlay fluorescence-bright-field images of coumarin-fluorescein-CNF at low magnification. The insets show higher magnification images of aggregates of FC-CNF.

- (14) Okahisa, Y.; Yoshida, A.; Miyaguchi, S.; Yano, H. *Compos. Sci. Technol.* **2009**, *69*, 1958–1961.
- (15) Biyani, M. V.; Foster, E. J.; Weder, C. *ACS Macro Lett.* **2013**, *2*, 236–240.
- (16) Glaied, O.; Dubé, M.; Chabot, B.; Daneault, C. *J. Colloid Interface Sci.* **2009**, *333*, 145–151.
- (17) Negishi, K.; Mashiko, Y.; Yamashita, E.; Otsuka, A.; Hasegawa, T. *Polymers (Basel, Switz.)* **2011**, *3*, 489–508.
- (18) Filpponen, I.; Argyropoulos, D. S. *Biomacromolecules* **2010**, *11*, 1060–1066.
- (19) Saito, T.; Kimura, S.; Nishiyama, Y.; Isogai, A. *Biomacromolecules* **2007**, *8*, 2485–2491.
- (20) Habibi, Y.; Goffin, A.-L.; Schiltz, N.; Duquesne, E.; Dubois, P.; Dufresne, A. *J. Mater. Chem.* **2008**, *18*, 5002–5010.
- (21) Liebert, T.; Heinze, T. *BioResources* **2008**, *3*, 576–601.
- (22) Goussé, C.; Chanzy, H.; Cerrada, M. L.; Fleury, E. *Polymer* **2004**, *45*, 1569–1575.
- (23) Filpponen, I.; Kontturi, E.; Nummelin, S.; Rosilo, H.; Kolehmainen, E.; Ikkala, O.; Laine, J. *Biomacromolecules* **2012**, *13*, 736–742.
- (24) Mangiante, G.; Alcouffe, P.; Burdin, B.; Gaborieau, M.; Zeno, E.; Petit-Conil, M.; Bernard, J.; Charlot, A.; Fleury, E. *Biomacromolecules* **2013**, *14*, 254–263.
- (25) Edwards, J. V.; Prevost, N.; Sethumadhavan, K.; Ullah, A.; Condon, B. *Cellulose* **2013**, *20*, 1223–1235.
- (26) Schyrr, B.; Pasche, S.; Voirin, G.; Weder, C.; Simon, Y. C.; Foster, E. J. *ACS Appl. Mater. Interfaces* **2014**, *6*, 12674–12683.
- (27) Navarro, J. R. G.; Bergström, L. *RSC Adv.* **2014**, *4*, 60757–60761.
- (28) Dong, S.; Roman, M. *J. Am. Chem. Soc.* **2007**, *129*, 13810–13811.
- (29) Edwards, J. V.; Prevost, N.; French, A.; Concha, M.; DeLucca, A.; Wu, Q. *Engineering* **2013**, *05*, 20–28.
- (30) Mahmoud, K. A.; Mena, J. A.; Male, K. B.; Hrapovic, S.; Kamen, A.; Luong, J. H. T. *ACS Appl. Mater. Interfaces* **2010**, *2*, 2924–2932.
- (31) Nielsen, L. J.; Eyley, S.; Thielemans, W.; Aylott, J. W. *Chem. Commun.* **2010**, *46*, 8929–8931.
- (32) Jennings, L. E.; Long, N. J. *Chem. Commun.* **2009**, 3511–3524.
- (33) Hüber, M. M.; Staubli, A. B.; Kustedjo, K.; Gray, M. H.; Shih, J.; Fraser, S. E.; Jacobs, R. E.; Meade, T. J. *Bioconjugate Chem.* **1998**, *9*, 242–249.
- (34) Bodunov, E. N.; Berberan-Santos, M. N.; Martinho, J. M. G. *Chem. Phys.* **2001**, *274*, 243–253.
- (35) Henriksson, M.; Henriksson, G.; Berglund, L. A.; Lindström, T. *Eur. Polym. J.* **2007**, *43*, 3434–3441.
- (36) Ax, J.; Wenz, G. *Macromol. Chem. Phys.* **2012**, *213*, 182–186.
- (37) Hon, D. N.-S.; Yan, H. *J. Appl. Polym. Sci.* **2001**, *81*, 2649–2655.
- (38) Metz, G.; Wu, X. L.; Smith, S. O. *J. Magn. Reson., Ser. A* **1994**, *110*, 219–227.
- (39) Kolodziejski, W.; Klinowski, J. *Chem. Rev.* **2002**, *102*, 613–628.
- (40) Bennett, A. E.; Rienstra, C. M.; Auger, M.; Lakshmi, K. V.; Griffin, R. G. *J. Chem. Phys.* **1995**, *103*, 6951–6958.
- (41) Chatterjee, P. K.; Stanonis, D. J. *J. Polym. Sci., Part A-1: Polym. Chem.* **1966**, *4*, 434–437.
- (42) Spivey, A. C.; Arseniyadis, S. *Angew. Chem., Int. Ed.* **2004**, *43*, 5436–5441.
- (43) Vilela, C.; Silvestre, A. J. D.; Gandini, A. *J. Polym. Sci., Part A: Polym. Chem.* **2013**, *51*, 2260–2270.
- (44) Tian, Q.; Yuan, Y. C.; Rong, M. Z.; Zhang, M. Q. *J. Mater. Chem.* **2009**, *19*, 1289–1296.
- (45) Shibata, M.; Teramoto, N.; Shimasaki, T.; Ogihara, M. *Polym. J.* **2011**, *43*, 916–922.
- (46) Gousse, C.; Gandini, A. *Polym. Int.* **1999**, *731*, 723–731.
- (47) Musto, P.; Martuscelli, E.; Ragosta, G.; Russo, P.; Scarinzi, G. *J. Mater. Sci.* **1998**, *33*, 4595–4601.
- (48) VanderHart, D. L.; Atalla, R. H. *Macromolecules* **1984**, *17*, 1465–1472.
- (49) Isogai, A.; Usuda, M.; Kato, T.; Uryu, T.; Atalla, R. H. *Macromolecules* **1989**, *22*, 3168–3172.
- (50) Kono, H.; Yunoki, S.; Shikano, T.; Fujiwara, M.; Erata, T.; Takai, M. *J. Am. Chem. Soc.* **2002**, *124*, 7506–7511.
- (51) Fujisawa, S.; Okita, Y.; Saito, T.; Togawa, E.; Isogai, A. *Cellulose* **2011**, *18*, 1191–1199.
- (52) SDBSWeb; <http://sdb.sriodb.aist.go.jp>.
- (53) Köhler, S.; Heinze, T. *Cellulose* **2007**, *14*, 489–495.
- (54) Grenier-Loustalot, M.-F.; Da Cunha, L. *Polymer* **1998**, *39*, 1833–1843.
- (55) Barazzouk, S.; Daneault, C. *Cellulose* **2011**, *19*, 481–493.
- (56) González-Béjar, M.; Frenette, M.; Jorge, L.; Scaiano, J. C. *Chem. Commun.* **2009**, 3202–3204.
- (57) Navarro, J. R. G.; Lerouge, F.; Micouin, G.; Cepraga, C.; Favier, A.; Charreyre, M. T.; Blanchard, N. P.; Lermé, J.; Chaput, F.; Focsan, M.; Kamada, K.; Baldeck, P. L.; Parola, S. *Nanoscale* **2014**, *6*, 5138–5145.
- (58) Navarro, J. R. G.; Lerouge, F.; Cepraga, C.; Micouin, G.; Favier, A.; Chateau, D.; Charreyre, M.-T.; Lanoë, P.-H.; Monnereau, C.; Chaput, F.; Marotte, S.; Leverrier, Y.; Marvel, J.; Kamada, K.; Andraud, C.; Baldeck, P. L.; Parola, S. *Biomaterials* **2013**, *34*, 8344–8351.
- (59) Hong, V.; Kislukhin, A. A.; Finn, M. G. *J. Am. Chem. Soc.* **2009**, *131*, 9986–9994.
- (60) Bhagwat, N.; Kiick, K. L. *J. Mater. Chem. C* **2013**, *1*, 4836–4845.